Proton−Water Charge-Transfer Processes: Follow-Up Study Using Configuration Interaction Calculations

F. Di Giacomo

Department of Chemical Engineering and Materials, University of Rome "La Sapienza", Via del Castro Laurenziano 7, 1-00161 Rome, Italy

F. A. Gianturco*

Department of Chemistry, The University of Rome, Città Universitaria, 00185 Rome, Italy

E. E. Nikitin

Department of Chemistry, Technion, Israel Institute of Technology, Technion City, Haifa 32000, Israel

F. Schneider

Weydermeyerstrasse 11, D-10178 Berlin, Germany

Received: April 21, 1999

In this paper we extend our previous study (Gianturco, F. A.; Raganelli, F.; Di Giacomo, F.; Schneider, F. *J. Phys. Chem.* **1995**, *99*, 64) on selective vibrational excitations in proton−water scattering experiments (Friedrich, B.; Niedner, G.; Noll, M.; Toennies, J. P. *J. Chem. Phys.* **1987**, *87*, 5256) presenting further MRD-CI calculations of specific "cuts" of the relevant potential energy surfaces (PESs). On the basis of the existence of crossing and avoided crossing features between PES's correlated to the $H + H_2O^+(\tilde{X})$ and $H^+ + H_2O$ and to $H^+ + H_2O$ and $H + H_2O^+(\tilde{A})$ asymptotic systems, two partially different mechanisms are proposed for proton−water charge-transfer processes leading to $H_2O^+(\tilde{X})$ or to $H_2O^+(\tilde{A})$. The model general predictions on the behavior of the total average vibrational energy transfer in the two channels as a function of scattering angle are shown to favorably compare with the experimental results, as also do the theoretical predictions on the size for the charge-transfer cross sections $\sigma_{CT}(\tilde{X})$ and $\sigma_{CT}(\tilde{A})$. The computed potential energy curves (PECs) for two of the most important lines of approach of protons to water molecules are further analyzed by using a generalized Heitler−London approximation, thereby affording us a better understanding of the physical reasons behind the general shapes of such "cuts". On the basis of symmetry arguments, the existence of a toroidal region is then surmised, which encircles water in its molecular plane through which a proton is to pass in order for the charge-transfer process $H^+ + H_2O \rightarrow H + H_2O^+(\tilde{X})$ to happen. The protonation of water, its nonadiabaticity and charge transfer aspects, and the dissociation channels of the bound oxonium are finally discussed, reinterpreting the computed PECs from these additional points of view.

1. Introduction

The pioneering high-resolution crossed-beam study of Toennies' group on proton scattering by water molecules[1] keeps stimulating theoretical studies on this important system. After an investigation we published[2] on the potential energy surfaces (PES) relevant to the interpretation of some of the experimental results there reported, a very recent work by Hedström et al.[3] uses electron nuclear dynamics theory (END) to compute differential cross sections for inelastic and charge-transfer reactions of H^+ and H_2O, comparing them with the experimental results.

In section 2 of the present paper, which is a continuation of our earlier paper in this journal, we first present new MRD-CI calculations of some of the potential energy curves (PECs) that will be shown to be related to the charge-transfer excitation (CTE) reactions:

$$H^+ + H_2O \rightarrow H + H_2O(\tilde{X}) \quad (1)$$

$$H^+ + H_2O \rightarrow H + H_2O^+(\tilde{A}) \quad (2)$$

where $H_2O^+(\tilde{X})$ and $H_2O^+(\tilde{A})$ represent oxoniumyl in its ground and first excited electronic states, respectively.

On the basis of our calculations, we propose an interpretation of the experimental results for the functional dependence of the total, mainly vibrational, average energy transfer $\langle \Delta E_{tot} \rangle$ into the $\tilde{X}$ and $\tilde{A}$ electronic states of H_2O^+ in reactions 1 and 2 as a function of the scattering angle ϑ. Considering the scattering cross sections $\sigma_{CT}(\tilde{X})$ and $\sigma_{CT}(\tilde{A})$ into the channels $\tilde{X}$ and $\tilde{A}$, we propose an explanation for (i) their weak dependence on ϑ for $\vartheta \leq 6°$ and (ii) the value of their branching ratio $\sigma_{CT}(\tilde{X})/\sigma_{CT}(\tilde{A})$.

In our earlier work[2] we studied different PECs for several possible directions of approach of H^+ to H_2O and we found out which one of them would mainly induce either stretching or bending vibrations of H_2O^+. We did also single out the

* To whom correspondence should be addressed. Fax: +39-6-49913305. E-mail: FAGIANT@CASPUR.IT.

10.1021/jp991313n CCC: $18.00
Published on Web 08/13/1999

directions of approach of H^+ to the oxygen atom in the plane of H_2O as being particularly effective in promoting process 1. In section 3, therefore, we additionally examine systematically the possible directions of approach of H^+ to H_2O, looking at the symmetries of the intermediate quasi-molecular complex $[H_2O-H]^+$ whose formation is surmised to be an essential step for explaining the energy loss spectra in ref 1. We additionally examine our MRD-CI PECs by qualitatively interpreting their patterns via a generalized Heitler−London (HL) approximation[4−6] and suggest from it that the H_2O molecule is surrounded in the molecular plane by a toroidal region of C_{2v} symmetry through which a proton must pass in order for reaction 1 to happen. Moreover, since the generalized HL approximation predictions significantly correlate singlet and triplet states arising from the asymptotic states $H + H_2O^+(\tilde{X}^2B_1)$ and $H + H_2O^+(\tilde{A}^2A_1)$, we also computed the triplet states curves and present here the new results.

In section 4 we make use of some of the PES profiles originally computed for the study of the CTE processes 1 and 2 (and for the interpretation of the fragmentation spectra of H_3O^+ [7,8]) to draw some information on the adjoining processes of water protonation, oxonium dissociation, and charge transfer and electron density changes that are likely to occur in the course of proton combination with the water molecule. We found that the protonation of water is a nonadiabatic process so that in order to form H_3O^+ directly in its ground-state, i.e., without going through excited electronic states, the proton must pass through a specific toroidal region that should be encircling water and should be located on its molecular plane.

After a discussion in section 5 on the limits of the validity of our results, we conclude by mentioning some recent results, closely related to ours, on the dissociation and protonation of NH_3, which is isoelectronic to H_3O^+.

2. MRD-CI Potential Energy Curves

In our previous investigation[2] we computed MRD-CI PES profiles for H^+ approaching H_2O along three different directions: (i) an "in-plane" approach in which the proton would draw nearer to the water in the plane of the molecule on the side of the oxygen atom and along the bisector of the HOH angle (a geometry of the $[H_2O-H]^+$ complex that we shall name "Y"); (ii) two "out-of-plane" approaches, one of which we called "perpendicular" with the proton approaching the oxygen perpendicularly to the molecular plane and the other "pyramidal" in which the proton would get near the oxygen along the direction of a lone pair. The calculations were done for those ground and excited electronic states of the $[H_2O-H]^+$ intermediate complex that correlate with the asymptotic states of $H^+ + H_2O$, with water in the ground or in the lower-lying excited states, or with $H + H_2O$, with oxoniumyl in its ground or in some of its excited electronic states.

Of the above states the most important ones are obviously the three lowest, i.e., the ones correlating to $H + H_2O^+(\tilde{X})$, $H^+ + H_2O(\tilde{X})$, and $H + H_2O^+(\tilde{A})$, in increasing energy order. We did search in ref 2 for crossings or avoided crossings among the three curves, i.e., for regions of possible nonadiabatic charge-transfer transitions, but we could find none in the "inner region" (1.6−2.4 a_o) of proton−water distances for any of the above orientations. In the "outer region" of distances we explored, between 2.4 and 6 a_o, we also could not find crossings or avoided crossings among the PECs for the "perpendicular" and "pyramidal" directions of approach, but a crossing was found at about 5 a_o for the planar "Y" geometry between the lowest two curves. The "Y" configuration was therefore singled out as one of the most important for inducing process 1.

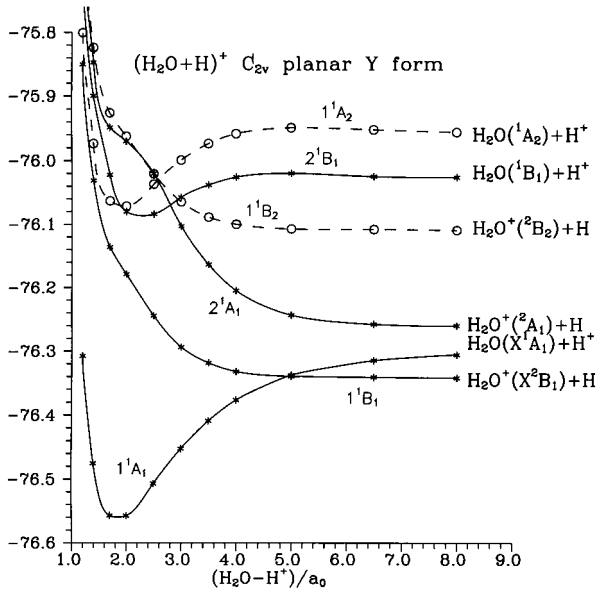

Figure 1. Computed MRD-CI energy values for the H^+−molecule interaction along the proton−H_2O distance in the "Y" form. The local singlet state symmetries of the $(H_3O)^+$ complex are marked along each PEC, while the various fragments in the asymptotic channels are marked on the extreme right for each curve. All values are in atomic units.

That the planar configuration of the $[H_2O-H]^+$ complex was particularly important for this system had already been suggested[2] as a result of some other considerations: (i) H_3O^+ in its ground-state configuration is in the form of a very flat pyramid of C_{3v} symmetry that, while undergoing umbrella motion, crosses an intermediate planar D_{3h} configuration; (ii) H_3O^+ in its first excited metastable electronic state was found to be planar with D_{3h} symmetry;[7] (iii) we found that the planar "Y" approach of H^+ to H_2O in the "inner region" of H^+-H_2O distances brings about an opening of the HOH angle of water, therefore leading to bending vibrations. The question then naturally arises as to what shape the PES profiles would have for planar approaches different from the "Y" mentioned above. We naturally chose the latter as the first to examine because in that configuration the ion−dipole interaction between H^+ and H_2O is the strongest. We also decided here to focus attention on the opposite planar configuration in which the proton approaches water from the side of the hydrogen atoms along the bisector of the HOH angle, a geometry we shall designate as "rhombic" and symbolized with "Rh".

We show in Figure 1 calculations for the "Y" configuration, which basically completes the work already shown in Figure 12 of ref 2. The calculations (which were done for a slightly different geometry, vide infra) are extended to smaller proton−water distances to show the repulsive branches of the PECs, and the curves have been smoothed by spline interpolation. Moreover, thanks to our recent calculations on the excited states of H_2O and H_2O^+ [9−11] we could unambiguously assign the correct asymptotic states to the curves. In Figure 2 we further show the same calculations but not for the "Rh" geometry.

2.1. Computational Details. For the present calculations we have chosen the geometry of water and of its ion, in both of the considered electronic states, to be with $r_{OH} = 1.86\ a_o$ and an HOH angle of 105°. The relevant elements of the basis set expansion, selection of configurations, and numerical details are the same as those already discussed in refs 2, 7, 9−11 and will therefore not be repeated here. The chosen geometry is neither the equilibrium geometry of water nor its ion in their ground electronic states but instead is the average of the

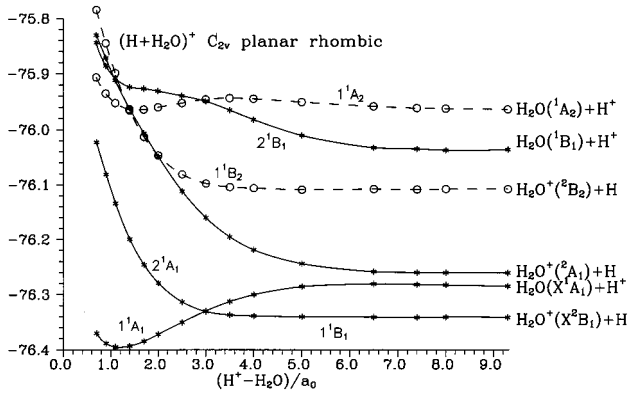

Figure 2. Same as in Figure 1 but for the planar rhombic arrangement.

TABLE 1

(a) Dissociation Energies and Dissociation Products for the Systems Studied in the Present Work (from Refs 2 and 12)

process	E (eV)
$H_3O^+ \rightarrow H_2^+ + OH$	9.69
$H_3O^+ \rightarrow H_3^+ + O$	8.09
$H_3O^+ \rightarrow H + H_2O^+(\tilde{A})^a$	7.28
$H_3O^+ \rightarrow H^+ + H_2O$	7.22
$H_3O^+ \rightarrow H_2 + OH^+$	7.28
$H_3O^+ \rightarrow H + H_2O^+(\tilde{X})$	6.25

(b) Electronic Configurations of the Neutral and Ionic Species Discussed in the Present Work (from Ref 14)

H_2O	(X^1A_1)	$(1a_1)^2$	$(2a_1)^2$	$(1b_2)^2$	$(3a_1)^2$	$(1b_1)^2$
H_2O^+	$(\tilde{X}^2B_1)$	$(1a_1)^2$	$(2a_1)^2$	$(1b_2)^2$	$(3a_1)^1$	$(1b_1)^1$
H_2O^+ [b]	$(\tilde{A}^2A_1)$	$(1a_1)^2$	$(2a_1)^2$	$(1b_1)^2$	$(3a_1)^1$	$(1b_1)^2$

[a] $D_{\infty h}$ symmetry. [b] C_{2v} symmetry.

computed equilibrium geometries of both these species, which are similar enough to each other.[9−11] The MRD-CI method has been applied to these calculations as in our earlier work in refs 2 and 7 and in the references reported there that describe the method. When either the proton or the hydrogen atom approaches the water target or the oxoniumyl ion in the "Y" geometry, the abscissa in both figures represents the distance between the proton (H) and the oxygen atom in water (H_2O^+). In the "Rh" approach the abscissa indicates the distance of H^+ (or H) to the center of mass of the two hydrogen atoms of H_2O (or of H_2O^+).

The energies of the three asymptotic states, given as dissociation energies of H_3O^+ in its ground state, are reported in Table 1. The value for the dissociation channel $H_3O^+ \rightarrow H + H_2O^+(\tilde{A})$ is now given as 7.28 eV following the sophisticated calculations of Brommer et al.;[12] i.e., it is only 0.06 eV above the 7.22 eV for the $H_3O^+ \rightarrow H^+ + H_2O$ channel with which it is almost degenerate. We have modified here the value in ref 2 in which we simply considered the energy difference between the two asymptotic states as due to the difference between the ionization potential of H and the second vertical ionization potential of H_2O[1].

The geometry of $H_2O^+(\tilde{A})$ used in our computation for the PEC correlated to $H + H_2O^+(\tilde{A})$ is not its linear one but is bent as described above. The asymptotic energy of the PES profile of the $H + H_2O^+(\tilde{A})$ system is then higher by about eight vibrational bending quanta with respect to the energy of H + linear $H_2O^+(\tilde{A})$, as may be easily seen from the figure or from Figure 1a in ref 10. In our calculations we did choose a bent geometry for $H_2O^+(\tilde{A})$ not only for the sake of simplicity but also because after the loss of an electron by the water molecules during the fast processes examined by the experiments, the $H_2O^+(\tilde{A})$ ion keeps for a brief instant the bent structure of the parent water molecule, and an excitation of about 8 bending quanta fits well in the range of the experimentally observed vibrational excitations of the $H_2O^+(\tilde{A})$ branch[1].

2.2. Average Vibrational Energy Transfer in $H_2O^+(\tilde{X})$ and $H_2O^+(\tilde{A})$. In this section we propose an interpretation for the following qualitative features of the curves reported in Figures 10 and 11 of ref 1. (i) The average total energy transfer $\langle \Delta E_{tot} \rangle_{\tilde{X}}$ in reaction 1 (which is mostly vibrational energy transfer $\langle \Delta E_{vib} \rangle_{\tilde{X}}$) is higher than the corresponding average energy transfer $\langle \Delta E_{FC} \rangle_{\tilde{X}}$, which can be calculated using the Franck−Condon (FC) factors of the $\tilde{X}$ state. (ii) $\langle \Delta E_{tot} \rangle_{\tilde{X}}$ remains virtually constant with increasing scattering angle ϑ. (iii) $\langle \Delta E_{tot} \rangle_{\tilde{A}}$ climbs instead, with increasing ϑ, from an initial value smaller than $\langle \Delta E_{FC} \rangle_{\tilde{A}}$ at $\vartheta = 0$ toward $\langle \Delta E_{FC} \rangle_{\tilde{A}}$ and reaching it for higher values of ϑ. (iv) The charge-transfer cross sections $\sigma_{CT}(\tilde{X})$ and $\sigma_{CT}(\tilde{A})$ show a weak dependence on σ for $\vartheta \leq 6°$ and are of the same order of magnitude.

A qualitative explanation that the ion $H_3O^+(\tilde{X})$ emerges from reaction 1 more vibrationally excited than would be predicted by a simple Franck−Condon picture, as suggested in ref 1, could come from considering that in a vibrationally excited product molecule the charge-transfer event is nearly resonant and therefore enhanced, according to the uncertainty principle, by a factor that is inversely proportional to the collision time. The collision time for a nonadiabatic transition is often so short (see ref 6, section 8.4) that the adiabatic restrictions are not very severe. Therefore, one could suggest an alternative explanation for the deviation from the FC prediction: if, prior to the nonadiabatic process, the H_2O molecule is adiabatically distorted by the charge−dipole interaction, then a transition close to the crossing line (the locus of the vertexes of the intersecting cones) would take place in a vertical manner between the distorted states of H_2O and the almost free states of $H_2O^+(\tilde{X})$. On the other hand, the equilibrium geometries of $H_2O^+(\tilde{X})$ and H_2O are already very close to one another and differ by having the $1b_1$ nonbonding MO either doubly or singly filled. It then follows that any adiabatic distortion of H_2O from its equilibrium configuration will increase the overlap between initial and final states. From simple electrostatic considerations one would therefore expect that the Coulomb field of H^+ would tend to slightly reduce the HOH angle and to slightly stretch the O−H bond distance to increase the dipole moment of H_2O when the intermediate $H + H_2O$ complex is formed in the "Y" configuration. A rather strong charge−dipole interaction between colliding species is anticipated already from the fact that a crossing distance of about 5 a_o can be extracted from the Y configuration PECs simply through the condition that the energy spacing between asymptotic channels in process 1 is mainly compensated by the charge−dipole interaction. The distortion of H_2O due to charge−dipole interactions in the $H^+ + H_2O$ "Rh" configuration would of course be the opposite of that in the "Y" case.

One of the most striking results from ref 1 was that the branching ratio for the electron transfer into the $\tilde{X}$ and $\tilde{A}$ states of H_2O^+ depends very weakly on ϑ for $\vartheta \leq 6°$ (see Figure 11 from ref 1). This would be hard to justify if the charge transfer into the $\tilde{X}$ and $\tilde{A}$ states were to occur by two completely different mechanisms. Since we already know that for the $\tilde{X}$ state the charge transfer proceeds via a curve-crossing mechanism[2] (more precisely, via a conical intersection), one wonders whether the same coupling could be responsible for the charge transfer into the $\tilde{A}$ state of H_2O^+. Since the crossing at 5 a_o between 1^1A and 1^1B_1 curves shown in Figure 1 can be qualitatively explained by the strong charge−dipole interaction,

showing a marked attraction at the entrance channel for the Y orientation, we should expect to have approximately the same amount of repulsion for the Rh orientation. Since the energy of the initial asymptotic state $1^1A_1(H^+ + H_2O)$ and that of the second final state $2^1A_1(H + H_2O^+(\tilde{A}))$ are very close to each other, the adiabatic PESs that correlate with them may experience a narrow pseudocrossing for the Rh orientation. If we were to neglect the resonance integral J (proportional to the overlap integral between the 1s AO of H and the a_1 MO of H_2O), the two PES will cross. This crossing, which is similar to the crossing of the covalent and ionic curves of NaCl or to the crossing in a harpooning reaction,[13] occurs at rather large relative distances (one can see from Figure 2 that this may happen at $R \geq 6\ a_o$). When the resonance interaction is taken into account, the crossing becomes an avoided crossing; i.e., the crossing between two diabatic PES of the same symmetry becomes an avoided crossing between two adiabatic PESs (vide infra). An important point to be made here is that the transition probability between two adiabatic vibronic states $|i\rangle$ and $|f\rangle$ will be given, in its simplest formulation, by the Landau−Zener prescription:

$$P_{if} = \exp\left(\frac{2\pi J^2 S_{if}^{\ 2}}{\hbar \Delta F v_R(b)}\right) \tag{3}$$

where S_{if}^2 is the overlap integral between vibrational functions for H_2O and H_2O^+, $v_R(b)$ is the radial velocity at the position of the seam, and b is the impact parameter. Although we expect that the collision dynamics would be very complicated, we can still argue that, for a given value of $v_R(b)$, the optimal path for the charge transfer would correspond to those final vibrational states of H_2O^+ for which the Landau−Zener exponent is less than 1. This yields an additional constraint for the overlap integral

$$S_{if} \leq \frac{\hbar \Delta F v_R(b)}{2\pi J^2} \tag{4}$$

If we now examine the experimental findings reported in Figure 10 from ref 1, we can say the following: with an increase in ϑ, b decreases; with a decrease of b for a given collision energy, $v_R(b)$ increases; with the increase of $v_R(b)$ the maximum value of S_{if}^2 that would be compatible with the constraint of eq 4 also increases. At sufficiently large ϑ, we would therefore get to a maximum value of S_{if}^2, which corresponds to the vertical transition. That is exactly what we see in the upper and lower panels of Figure 10 in ref 1. Thus, we can qualitatively explain the difference between the angular dependence of the energy transfer into the $(\tilde{X})$ and $(\tilde{A})$ states of H_2O^+ as a simple consequence of the fact that the charge transfer $H^+ + H_2O \rightarrow H + H_2O^+(\tilde{X})$ occurs via the conical intersection while the charge transfer $H^+ + H_2O \rightarrow H + H_2O^+(\tilde{A})$ occurs via the avoided crossing and over a broader range of distances between partners. An additional test of this mechanism would come from the dependence of the energy-transfer curves $\langle \Delta E_{tot}(\vartheta,\tilde{X})\rangle$ and $\langle \Delta E_{tot}(\vartheta,\tilde{A})\rangle$ on the collision energy. For the process $H^+ + H_2O \rightarrow H + H_2O^+(\tilde{X})$ we do not expect an appreciable energy dependence of $\langle \Delta E_{tot}(\vartheta,\tilde{X})\rangle$. On the other hand, for the process $H^+ + H_2O \rightarrow H + H_2O^+(\tilde{A})$, which is constrained by inequality 4, an increase of energy (a velocity increase) will cause a faster reaching of its asymptotic Franck−Condon limit for the quantity $\langle \Delta E_{tot}(\vartheta,\tilde{A})\rangle$ and, generally, to higher values of this quantity for higher collision energies. All the above qualitative estimates indeed appear to be consistent with the experimental data presented in Figure 10 of ref 1.

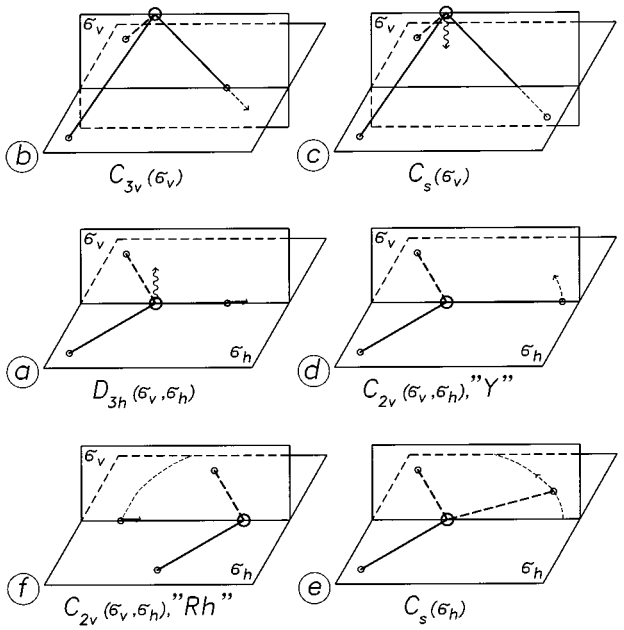

Figure 3. Schematic representation of the symmetry changes induced in the $[H_3O]^+$ system by selective deformations via different nuclear displacements. See text for definitions.

It is to be emphasized here that the difference between the conical crossing and the avoided crossing is that in the former case there always exists a configuration where the nonadiabatic transition probability is unity or close to it, while in the latter case the maximum transition probability is still proportional to the Landau−Zener exponent. As a result, the mean transition probability for the conical intersection depends weakly on all the parameters of eq 3, while for the avoided crossing the mean transition probability may strongly depend on them because of the Landau−Zener exponent. Finally, both charge-transfer channels go basically via the same Landau−Zener mechanism; a conical intersection is an avoided crossing seam for a single point (the vertex of the cone), and a pseudocrossing is instead an avoided crossing everywhere. It is therefore not very surprising to find that the branching ratio between the cross sections in the two channels, shown by the experiments of ref 1, indicates that they do not differ by orders of magnitude but are rather fairly close to one another.

3. Nuclear Symmetries of the $[H_2O-H]^+$ Complex

In view of their use later on in this work, we will briefly examine systematically the possible symmetries of the $[H_2O-H]^+$ "complex", i.e., the intermediate "quasi-molecular states"[1] $H^+ + H_2O$, $H + H_2O^+(\tilde{X})$ and also $H + H_2O^+(\tilde{A})$ with $H_2O^+(\tilde{A})$ in a vibrationally excited, bent geometry. The following analysis obviously also includes, in particular, the possible geometries of hydroxonium, H_3O^+.

A system of four atoms, as in the $[H_3O]^+$ complex, does not belong in general to a specific point-group symmetry. Therefore, one has to consider a subset of configurations that are likely to display a certain level of symmetry. We begin with the highest symmetry of the $[H_3O]^+$ complex, i.e., the one corresponding to a planar arrangement of the four partners in which the hydrogen atoms form an equilateral triangle and the oxygen atom is at the center of this triangle. The point group of this configuration is D_{3h}, and it encompasses several symmetry elements. Two of them, which are of interest to us, are the symmetry planes σ_h and σ_v shown in Figure 3a.

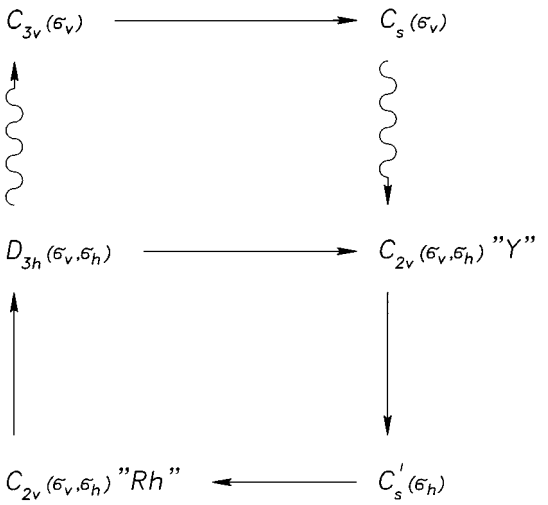

Figure 4. Further scheme of nuclear symmetry changes in the $[H_3O]^+$ system induced by H displacements (solid arrows) and by O displacements (wavy arrows).

When atomic species are displaced from the most symmetrical configuration, the D_{3h} symmetry will be lowered. By pulling the oxygen out of the plane of the hydrogen nuclei and in a direction perpendicular to it, we arrive at the configuration of a trigonal pyramid (Figure 3b) with the point group C_{3v}. If one of the protons is pulled away from the present equilibrium position while it is kept in the σ_v plane passing through it, the symmetry of the pyramid changes from C_{3v} to C_s, as shown in Figure 3c.

On the other hand, when the molecule undergoes the umbrella motion, the oxygen atom goes through the plane defined by the hydrogen nuclei, thereby creating an intermediate configuration of the four atoms in D_{3h} symmetry as in Figure 3a.

If one of the protons is pulled away from its equilibrium position in this last configuration while it is kept in the σ_h plane and in the σ_v plane to which it belongs, the form of the triangle defined by the hydrogen nuclei changes from equilateral to isosceles with the symmetry now changed to C_{2v} (Figure 3d). We did designate as "Y" this last planar configuration of the $[H_3O]^+$ complex. We should also consider the further possibility of displacing one of the protons into an arbitrary position of the initial plane of $[H_3O]^+$. In this case the symmetry of the final configuration is in general C_s', the symmetry of the system being that of reflection in the plane containing the four atoms, where the three hydrogen nuclei would form in general a scalene triangle, as shown in Figure 3c.

An interesting limiting planar configuration is that in which the proton lies on the axis bisecting the HOH angle on the side of the other two hydrogen atoms, as seen in Figure 3f. We referred above to this configuration as the "rhombic" one, symbolizing it with "Rh".

Finally, no symmetry element is present in a general C_1 configuration of the complex in which one would end up when displacing the proton from the configuration C_s' out in directions perpendicular to the plane. In Figure 4 the above symmetries and the described displacements are schematically summarized. The wiggly and straight arrows are used to indicate the displacements of oxygen and hydrogen species, respectively.

3.1. Shapes of the Lower-Lying PES for $[H_2O-H]^+$: Qualitative Analysis. In this section we shall examine the three lowest PES profiles for $[H_2O-H]^+$ in terms of the generalized Heitler−London (HL) approximation coupled with the asymptotic estimates of the exchange and resonance integrals appearing in it.[4−6] This will afford us (i) the possibility of qualitatively predicting the shapes of the PECs as well as (ii) a physical understanding of the basic interactions between protons and water molecules or of hydrogen atoms and the oxoniumyl ion. Moreover, (iii) we will show that this analysis, together with the above symmetry considerations, will lead to the finding of a general condition for reaction 1 to happen.

As anticipated in the Introduction, we present in Figures 5 and 6 the triplet states MRD-CI calculations for the Y and Rh configurations of the intermediate complex corresponding to the singlets of Figures 1 and 2. The predictions of the shapes of singlet and triplet curves using the generalized HL approximation method will be compared with the shapes of the curves actually computed, thus allowing a check of the HL predictive quality for this system.

A peculiarity of the $[H_2O-H]^+$ complex is that, as shown by our earlier calculations,[2,7] the three lower-lying asymptotic states $H(1s) + H_2O^+(\tilde{X}^2B_1)$, $H^+ + H_2O(\tilde{X}^1A_1)$, and $H(1s) + H_2O^+(\tilde{A}^2A_1)$ are close to each other and noticeably separated from the other higher states. This suggests that at large distances between fragments the main relevant PESs can be qualitatively analyzed in terms of configuration interaction mixings between only those configurations of the $[H_3O]^+$ system that are generated by the basis of the dominant configurations describing the fragments in each of the above asymptotic channels. One should also remember, however, that such a simplified picture is not likely to be valid when the partners undergo the stronger chemical interactions that exist in the inner region of nuclear configurations and that have been analyzed, therefore, by our MRD-CI calculations.

To facilitate the discussion, we now introduce a body-fixed frame attached to H_2O in its C_{2v} configuration, as in Figure 7. We take the molecular plane as the *xz* plane and point the *z* axis originating at the O nucleus opposite to the two H atoms. In this reference frame the polar coordinates of an incoming proton (or of an hydrogen atom) are r, ϑ, φ. Since in the following we shall further refer to the molecular orbitals of water and to their symmetries,[14] we remind the readers at this point of their qualitative and bonding features by showing them in Figure 8. In Table 1 (bottom) the electronic configurations of the relevant water partners are also given.

To begin with, we consider the C_{2v} symmetry and the two geometries Y and Rh that we already considered in our calculations for the approaching hydrogen species (H^+ and H). We shall discuss first the possible behavior of the diagonal matrix elements V_{11}, V_{22}, and V_{33} for the electronic configurations that correspond to the separated fragments (the diabatic interaction) in the order of their increasing asymptotic energies.

A. The asymptotic interaction V_{11} between H_2O^+-$(2a_1^2\,1b_2^2\,3a_1^2\,1b_1,\tilde{X}^2B_1)$ and H(1s), in the Y and Rh geometries, contains the electronic charge-induced dipole interactions,

$$V_{el} \propto -\frac{\alpha}{2R^4}$$

which is attractive both for the Y and for the Rh geometries. Owing to the low polarizability of the H atom, this interaction becomes weak at intermediate to large distances. Furthermore, at closer quarters, the additional exchange interaction is given by a sum of the two-electron exchange integrals involving the 1s AO of H and one of the filled MOs of H_2O^+. In analogy to

the case of two interacting atoms, we can surmise that the molecular exchange integral is also positive for the orbitals of the same symmetry and negative for orbitals of different symmetry. The integrals involving orbitals of different symmetries are also smaller by a factor a_o/R.[6]

In qualitative terms, we can therefore see that each of the exchange integrals is proportional to an exponential factor exp$(-\gamma R/a_o)$, where γ depends on the ionization potential of a particular MO of H_2O and of the 1s AO of H.[6] For our present qualitative discussion it will suffice to take the ionization potential of all the orbitals to be the same and equal to 0.5 au, which makes $\gamma = 2$. Note that the exp $(-2R/a_o)$ dependence of the exchange integrals is the same as that which gives the singlet−triplet splitting in the textbook example of the hydrogen molecule (see ref 15, the footnote to the problem discussed in section 81).

We therefore find the following contributions to occur for the exchange interaction between $H_2O^+(2a_1^2\ 1b_2^2\ 3a_1^2\ 1b_1,\tilde{X}^2B_1)$ and H(1s):

(i) repulsion between the doubly filled $2a_1$ MO and 1s AO; (ii) weak attraction between doubly filled $1b_2$ MO and 1s AO; (iii) repulsion between the doubly filled $3a_1$ MO and 1s AO; (iv) weak repulsion between the singly filled $1b_1$ MO and 1s AO for the singlet state and weak attraction in the triplet state interaction. Hence, we expect that out of the two states arising from the $(2a_1^2\ 1b_2^2\ 3a_1^2\ 1b_1,1s)$ configuration, the diabatic triplet state $^3B_1$ will lie below the diabatic singlet state $^1B_1$ but also that the singlet−triplet splitting will be hardly noticeable on the background of the overall repulsion occurring at the shorter interparticle distances, as shown here in Figures 9a and 10a where the qualitative patterns of the diabatic potential energy curves $V(R)$ are schematically depicted. For the $H + H_2O^+(\tilde{X})$ system there is no qualitative reason, therefore, to find the interaction in the Rh geometry to be markedly different from that in the Y geometry.

B. If we now turn our attention to the interaction V_{22} between $H_2O(2a_1^2\ 1b_2^2\ 3a_1^2\ 1b_1^2,\tilde{X}^2\ ^1A_1)$ and H^+, we see that it corresponds to a strong charge−dipole interaction, $V_{el} \propto 1/R^2$, which is attractive for the Y geometry and repulsive for the Rh one. There is no exchange interaction between fragments, since the 1s orbital of the H atom is vacant; the state arising from this configuration can be classified as being a $^1A_1$ diabatic state (see Figures 9a and 10a).

C. In the asymptotic interaction V_{33} between H_2O^+-$(2a_1^2\ 1b_2^2\ 3a_1^2\ 1b_1^2,\tilde{X}^2\ ^1A_1)$ and H(1s), we find once more the charge-induced dipole interaction to be very weak, and therefore, it can be ignored. As for the exchange interaction at shorter distances, we can list the following contributions: (i) repulsion between the doubly filled $2a_1$ MO and 1s AO; (ii) weak attraction between doubly filled b_2 MO and 1s AO; (iii) attraction between the singly filled $3a_1$ MO and 1s AO for the singlet state; (iv) repulsion for the triplet state. We therefore expect that out of the two states arising from the $(2a_1^2\ 1b_2^2\ 3a_1\ 1b_1^2,1s)$ configuration the diabatic triplet state $^3A_1$ will lie above the diabatic singlet state $^1A_1$ and that the singlet−triplet splitting will be noticeable on the background of the overall repulsion at rather short interparticle distances. This repulsion is expected to be weaker than for the $^1B_1$ state. Once again, the interaction should be qualitatively the same for both the Y and Rh geometries. Figures 9a and 10a report a pictorial view of the predicted patterns.

The main feature of the patterns of diabatic potential surfaces that emerges from the above considerations chiefly comes from the long-range behavior of the $^1A_1$ PES; we should therefore expect a crossing between $^1A_1$ and $^1B_1$ PES in the Y configuration (strong charge−dipole attraction in the $^1A_1$ state) and a crossing between the two singlet $^1A_1$ PESs in the Rh configuration (strong charge−dipole repulsion in the $^1A_1$ state).

However, this picture will be considerably modified when one further takes into account the charge-transfer interaction V_{23} between two diabatic states of $^1A_1$ symmetry as graphically represented by the springy double arrows in Figures 9a and 10a. This interaction could qualitatively be expressed via the one-electron resonance integral between the 1s AO of the H atom and the $3a_1$ MO of the H_2O molecule, which is proportional[5] to exp$(-R/a_o)$. Once again, we refer to a simple textbook example, in this case to the H_2^+ ion (see ref 15, problem to section 81). Note that the exponent for the resonance interaction is one-half that for the exchange interaction. This means that the resonance interaction is more likely to show itself at much larger intermolecular distances, where the exchange interaction can be largely neglected.

Thus, at large internuclear distances the adiabatic PES can be found through the eigenvalues W_1, W_2, W_3 of the model Hamiltonian matrix given in eq 5.

$$H = \begin{pmatrix} V_{11} & 0 & 0 \\ 0 & V_{22} & V_{23} \\ 0 & V_{23} & V_{33} \end{pmatrix} \tag{5}$$

The main effect of the resonance integral is to further separate the adiabatic PES, W_2, and W_3 that arise from the two diabatic PES, V_{22} and V_{33}. This is pictorially shown by Figures 9 and 10 when comparing there the lower and upper panels a and b. For the Y geometry we would expect that this "push-out" effect will increase the attractive character, which is pictorially shown by the adiabatic 1^1A_1 state W_2, compared to its diabatic counterpart and also increase the repulsive character of the adiabatic 2^1A_1 state W_3. This feature will have two consequences. First, the increased separation will favor an earlier crossing of 1^1A_1 and 1^1B_1 potential curves because of the concerted action of the charge−dipole and the exchange contributions. Second, the repulsion in the adiabatic state 2^1A_1 will be stronger than in the adiabatic $^3A_1$ state; i.e., the passage from the diabatic to the adiabatic picture reverses the ordering of the singlet and triplet states arising from the H_2O^+-$(2a_1^2\ 1b_2^2\ 3a_1 1b_1^2,\tilde{A}^2A_1)$ and H(1s) asymptotic states. On the other hand, for the Rh geometry, the "push-out" effect will change the crossing of the two $^1A_1$ PESs into an avoided crossing between 1^1A_1 and 2^1A_1 adiabatic PESs. A rough estimate of the avoided crossing spacing may be obtained the following way. According to the asymptotic method,[5] the resonance interaction is largely determined by the electronic wave function of the two partners in a region at the midpoint between them. Now, to a first approximation, the asymptotic behavior of the $3a_1$ MO may look like a linear superposition of two 1s AO of H atoms (see Figure 8). Therefore, it is tempting to identify the avoided crossing spacing with the value caused by the resonance splitting between the two lowest states in H_2^+. The analytical expression for the latter is $(4/e)R\ \exp(-R)$ (see ref 15, problem to section 81), which yields 0.009 au at $R = 7\ a_o$, the most likely value of the expected crossing distance along the two adiabatic profiles. The behavior of the lower adiabatic PES $^1A_1$ to the left of the avoided crossing region will be governed by the attractive charge-transfer interaction and, at smaller distances, by the repulsive exchange interaction. The resonance integral can then bring about the crossing of the 1^1A_1 PES with the 1^1B_1 PES, while the behavior of the upper

adiabatic PES 2^1A_1 will be governed by the repulsive charge−dipole and resonance interactions.

The symmetry properties of the MOs, which are crucial for the above discussion, are related to the reflection through the system plane and not to any other symmetry operation of the C_{2v} point group. Therefore, all the above considerations about the qualitative patterns of the adiabatic PES remain valid for any arbitrary planar configuration. We thus expect that in the plane of the H_2O molecule there should exist a curve that can connect the two crossing points in the Y and Rh configuration and that represents the crossing seam between the lowest two singlet adiabatic PES of the planar $[H_2O-H]^+$ system, one belonging to the $^1A'$ and the other to the $^1A''$ symmetry species of the C_s point group.

For a nonplanar geometry there will be a nonzero one-electron resonance integral V_{12} between the 1s AO of H and the b_1 MO of H_2O, and the energy matrix becomes in turn the one of eq 6

$$\mathbf{H} = \begin{pmatrix} V_{11} & V_{12} & 0 \\ V_{12} & V_{22} & V_{23} \\ 0 & V_{23} & V_{33} \end{pmatrix} \tag{6}$$

where all the matrix elements depend on the orientation of the vector $\hat{r}$ of the incoming H^+ with respect to a molecular frame referenced to the rigid framework of H_2O. We then expect, according to the symmetry of the $1b_1$ MO of H_2O, that V_{12} would be proportional to cos γ where γ is the angle between $\hat{r}$ and the normal to the H_2O plane, which yields[5] $V_{12} \propto \sin\vartheta \sin\varphi$. The in-plane orientation of $\hat{r}$ means $\varphi = 0$ or $\varphi = \pi$, which yields $V_{12} = 0$. This condition defines the crossing seam for the planar configuration.

For a slightly nonplanar geometry, the crossing line between the two lowest potential surfaces becomes the avoided crossing, or an avoided crossing seam. If we define the eigenvalues of the Hamiltonian (eq 6) to be the adiabatic PESs (in the order of increasing energy), U_1, U_2, U_3, then the adiabatic PES U_1 in the planar geometry consists of W_2 to the left from the crossing point and of W_1 to the right of it. In the new nomenclature, however, we should speak no more of crossings but rather about touching or confluent points: the two lower PES of the H_3O^+ planar configuration, U_1 and U_2, touch each other along a line drawn by the $\hat{r}$ vector in this plane (the seam).

It is now clear that the formation of a complex $[H_2O-H]^+$ in its ground electronic state becomes possible only as a result of a transition from the first excited potential energy surface. The probability of this nonadiabatic transition is appreciable only if the system goes into the potential well through a region centered at the touching curve and the width of this region depends on the velocity of the relative motion of the fragments. It becomes zero in the adiabatic approximation. *One can therefore say that the H_2O molecule when interacting with H^+ is encircled by a toroidal region of C_{2v} symmetry, which lies in the plane of the molecule, and the crossing of this region by the incoming proton or by the outgoing H atom is a necessary condition for the appearance of an asymptotic channel that results in the ground electronic state of H_2O^+ and an H atom. The nonadiabatic nature of the charge transfer shows itself in the fact that the width of this toroid goes to zero with decreasing velocity of the impinging proton.*

3.2. Computed vs Predicted PECs. Inspection of Figures 1 and 2 reveals an interesting qualitative similarity between the lowest three MRD-CI adiabatic curves and the general patterns, which, predicted on the basis of the previous simple HL theoretical considerations, are schematically depicted in Figures 9b and 10b. We can therefore safely ascribe the most important features of the ab initio potential energy curves (PECs) to the following types of interactions.

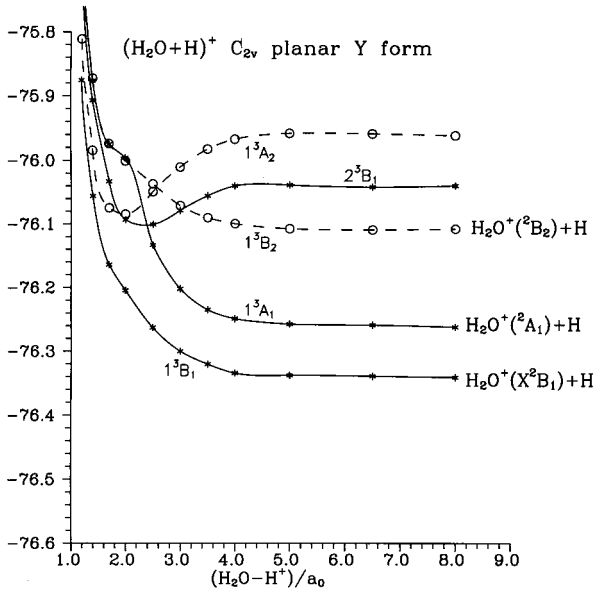

Figure 5. Same as in Figure 1 but for the triplet state symmetries of the equivalent PEC in the "Y" arrangement shown in that figure.

(i) In Figure 1 the crossing between $^1A_1$ and 1^1B_1 curves is due to the combined action of attractive electrostatic (mainly charge−dipole) and resonance interactions. The initial repulsion in the 2^1A_1 state is due to repulsive resonance interaction. At smaller distances, however, the exchange interaction contributes to the repulsion in all three states. The crossings at smaller distances correlate to the degeneracies of the electronic states of planar hydroxonium in D_{3h} symmetry (see Figure 5 from ref 2). Our system of Y geometry and C_{2v} symmetry would go into that of D_{3h} symmetry where the HOH angle of the water moiety opened to 120°. We would then reach the crossings of Figure 5 in ref 2 at $R = r_{OH} = 1.86\ a_o$.

(ii) In Figure 2 the pseudocrossing between 1^1A_1 and 2^1A_1 curves can be attributed to the resonance interaction. The small splitting between these curves (about 0.02 au at $R \cong 7\ a_o$) qualitatively agrees with our estimate of 0.009 au (vide supra) and provides some assurance on the likely correctness of our qualitative analysis. At smaller distances the 1^1A_1 curve crosses the 1^1B_1 curve because of the attractive resonance interaction for the former state. As in Figure 1, the outer repulsion in the 2^1A_1 state is due to repulsive resonance interaction, while at smaller distances the exchange interaction dominates the repulsion in all three states. We also see various multiple crossings of excited PESs in the range 1−2 au of distance. It would be nice to possibly assign these crossings to the broken higher symmetry D_{4h} as in the case of the Y geometry. In fact, a glance at the Rh geometry in this region suggests that the symmetry of a distorted square is obtained when *one treats the O atom as if it were an H atom* (see Figure 11). Such a simplification may be possible for electronic states under discussion because the ionization potential of the valence shell of the O atom is very close to the ionization potential of the H atom. In other words, a single electron located in the outer region of the wave function may not see much difference between O^+ and H^+ as attractive centers. The important difference between Y and Rh geometry is, however, that in the former case one can, by adjusting angles and lengths, bring the isosceles triangle formed by the three H nuclei to the D_{3h} shape as in Figure 11a, while in the latter

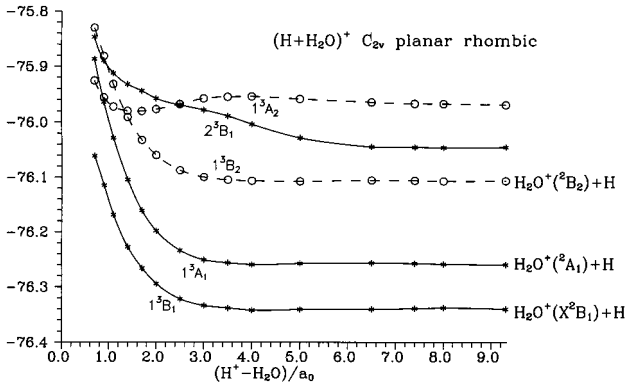

Figure 6. Same as in Figure 2 but for the triplet state symmetries in the planar rhombic arrangement and for the lower-lying electronic states.

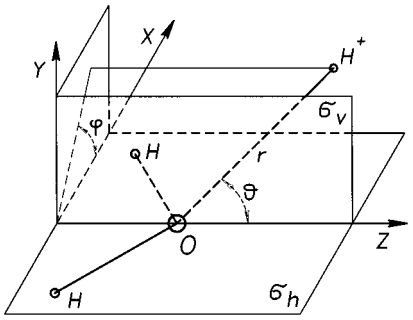

Figure 7. 3D orientation of the $\hat{r}$ vector associated with the incoming proton with respect to the body-fixed reference frame of the H_2O partner.

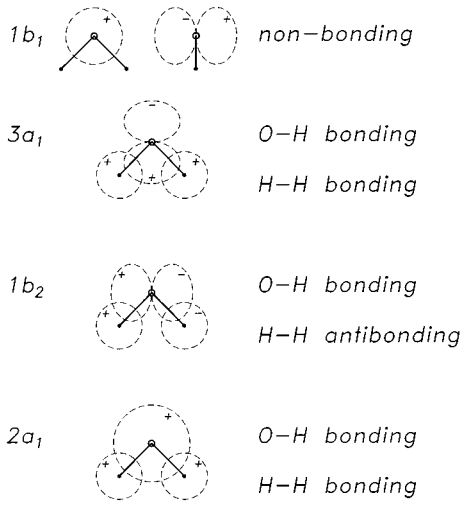

Figure 8. Qualitative shape of the spatial distributions for the four highest occupied MO's of the water molecule (see Table 1).

case it is not possible to bring the system to the exact D_{4h} symmetry (see Figure 11b).

(iii) A comparison of Figure 5 with Figure 1 shows that the triplet $^3B_1$ curve lies slightly below the singlet $^1B_1$ curve. This agrees with the prediction of our previous diabatic modeling (Figure 9), which, for these symmetries, is not altered by the resonance interaction. The triplet $^3A_1$ curve lies noticeably below the singlet 2^1A_1 curve. This disagrees with the prediction of the diabatic approach, since, when going from a diabatic to an adiabatic description, the 2^1A_1 curve is strongly pushed upward by the resonance interaction, and therefore, the 2^1A_1 adiabatic curve should lie above the 1^3A_1 adiabatic curve. Finally, from the results reported in Figure 6 we see that the pattern of the

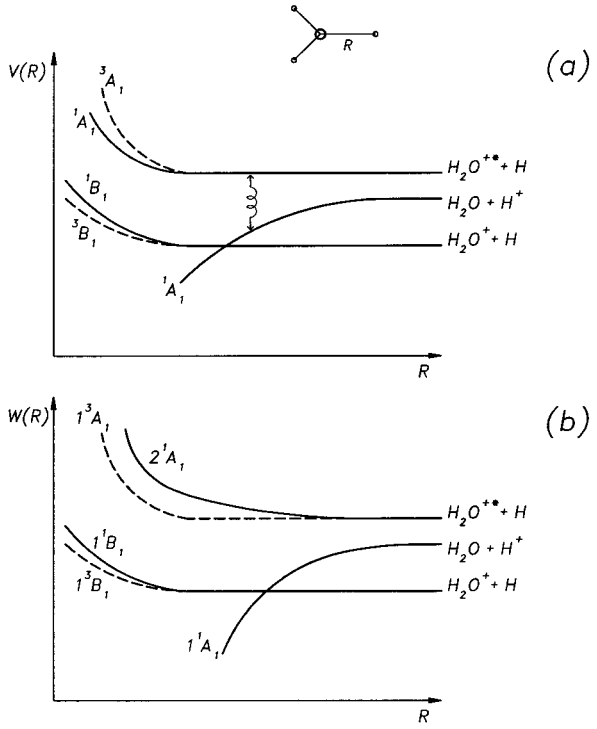

Figure 9. Diabatic (a) and adiabatic (b) qualitative patterns for the three lowest PES profiles and for the Y configuration of the partners, as predicted by the generalized Heitler−London approximation. The V_{23} charge-transfer interaction between the diabatic states of $^1A_1$ symmetry is symbolized with a springy double arrow connecting them.

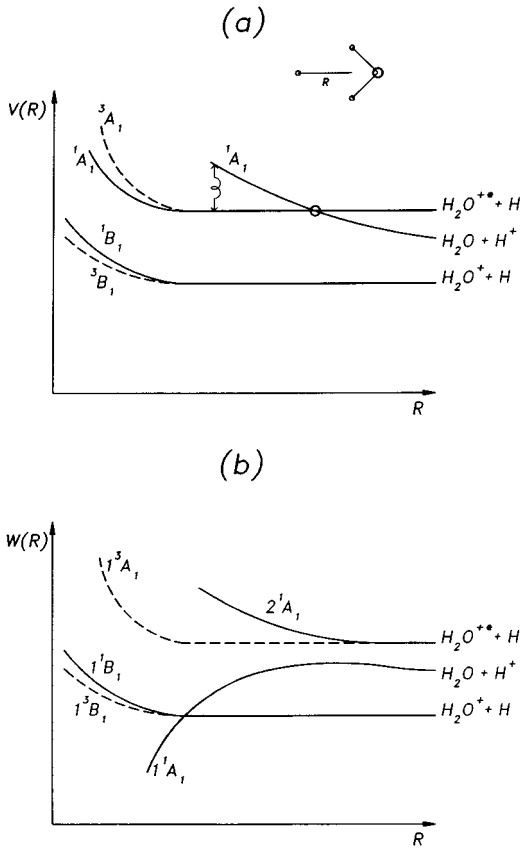

Figure 10. Same as in Figure 9 but for the planar rhombic arrangement.

curves in this figure is qualitatively similar to that of Figure 5, as previously predicted.

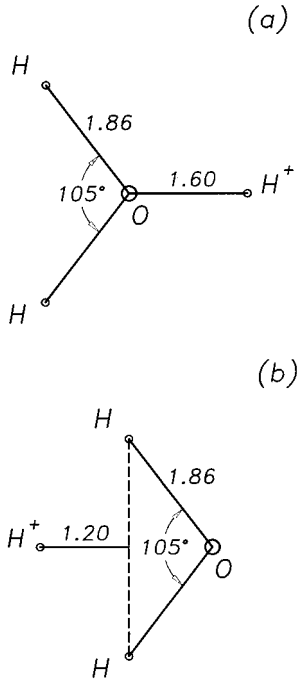

Figure 11. Schematic presentation of the specific geometries corresponding to the crossing regions in the planar arrangements for the proton approach to the H_2O partner: (top) "Y" arrangement; (bottom) rhombic arrangement.

4. Protonation of H_2O and the Deprotonation−Dehydrogenation of H_3O^+

It was with the aim of achieving a better understanding of processes 1 and 2 that the above special MRD-CI PECs were computed. We shall now examine them from a different viewpoint, looking at the adjoining problems of water protonation

$$H^+ + H_2O \rightarrow H_3O^+ \tag{7}$$

and of the homolytic and heterolytic bond dissociations of the hydroxonium ion formed in reaction 7:

$$H_3O^+ \rightarrow H^\bullet + H_2O^{\bullet +} \tag{8}$$

$$H_3O^+ \rightarrow H^+ + H_2O: \tag{9}$$

When the proton H^+ approaches a neutral molecule and dissipation channels are available to dispose of the excess relative energy, two general electronic pathways for the formation of an adduct ion are possible. If the electronic energy level of the $H^+ + M$ system at infinite separation between the fragments lies below the energy level of the $H + M^+$ system, the electronic state of the $H^+ + M$ system adiabatically correlates with the ground electronic state of the ion $(MH)^+$. On the other hand, if the electronic energy level of the separated $H^+ + M$ system lies above the energy level of the $H + M^+$ system, the electronic state of the $H^+ + M$ system adiabatically correlates, in general, with an excited electronic state of the ion $(MH)^{*+}$. Of course, in the latter case there are likely to exist special reaction paths along which it is possible to pass smoothly from the electronic state that correlates with $H^+ + M$ to the ground electronic state of $(MH)^+$. This passage, which continuously leads from the excited electronic state of the fragments to the ground electronic state of a combined system, can be called adiabatic in the sense of smooth dependence of the electronic wave function in the nuclear coordinates along this path. At the same time, this passage can also be called diabatic, since it brings the final system from the upper potential surface to the lower one. This controversial nomenclature is simply related to the fact that it was devised without taking into account all the complicated features of the celebrated Teller conical crossing.[16] Nowadays, the properties of a multidimensional conical intersection are well documented in standard texts (e.g., refs 14, 17, 18), and one usually calls the lower and upper surfaces the adiabatic ones. If the velocities of the nuclei are low enough, the nonadiabatic transitions between adiabatic PESs occur in regions located close to the conical intersection. Within this wording, the formation of a protonated molecule in its ground electronic state under conditions where the ionization potential of the molecule, I_M, is less than that of the hydrogen atom, I_H, constitutes an electronically nonadiabatic event. This is true in particular in the case of the protonation of water (eq 7) for which $I_M = 12.62$ eV and $I_H = 13.95$ eV.

What the above discussion means is that it is not possible for the $H^+ + H_2O$ asymptotic system to reach a bound state configuration of H_3O^+ in its ground electronic state by nuclear motion on a single adiabatic potential energy surface without passing through a crossing or an avoided crossing of PESs. This general property will now be illustrated in a heuristic way following possible protonation paths with the proton approaching water from different directions, looking at the accompanying charge transfer and electron density changes.

The two lowest PECs of Figure 1 let us follow a possible protonation pathway of H_2O in the special case when the proton approaches the water molecule in the plane of the molecule following the Y geometry. The strong ion−dipole interaction between H^+ and H_2O will tend to reduce the HOH bond angle and to lower the PEC, which correlates to $H^+ + H_2O$ toward the PES, which asymptotically correlates to $H + H_2O^+(\tilde{X})$, as already discussed above and as one sees in Figure 1. At a distance R_o of about 2.5 Å the two PECs, belonging to different symmetries, cross. In the neighborhood of the crossing electron transfer may occur, thereby leading to vibrationally excited oxonimyl $H_2O^+(v; \tilde{X})$ in its ground electronic state. Following the PES, with H now getting still closer to H_2O^+, a covalent bond may form between $H^\bullet$ and $H_2O^{\bullet +}$, leading to oxonium in its first excited electronic state, $H_3O^+(2^1A_1)$, in a planar D_{3h} configuration as given by a representative point at the bottom of the 2^1A_1 curve shown in Figure 5 of ref 7. If the charge is not transferred, the $H^+ + H_2O(\tilde{X})$ system will follow the lowest PES and the proton, approaching water, will withdraw electron density particularly from the $3a_1$ MO of H_2O (see Figure 8) with an opening effect in the HOH bond angle of H_2O (see Walsh diagrams in ref 19) and a gradual transformation of an oxygen lone pair into a bonding pair.[20] The system will therefore pass through the representative point of D_{3h} symmetry on the col of curve $\tilde{X}^1A_1$ (Figure 3 of ref 7) and will then relax to $H_3O(\tilde{X})$ in the minimum energy C_{3v} configuration if left to evolve spontaneously on the PES; i.e., it will end up in one of the two wells of that curve.

Recalling the discussion in section 3 on a toroidal region through which an outgoing proton is to pass in order for the $H + H_2O^+$ system to appear, we see that the above observations are by no means restricted to a planar Y C_{2v} symmetry of the $[H_3O]^+$ complex. As a matter of fact, a direct protonation of water—by which we mean a protonation process leading to H_3O^+ in its ground electronic state with the system moving on the PES correlated to $H^+ + H_2O$—is only possible if the $[H_2O-H]^+$ complex assumes an arbitrary intermediate planar or near-

planar configuration while the proton passes through the above tubular neighborhood of the full, multidimensional interaction.

Let us now consider the protonation path symmetrical to the one examined above in which the proton approaches water in Rh geometry. The electrostatic ion−dipole interaction is now repulsive and will tend to increase the HOH bond angle. The PEC asymptotically correlating to $H^+ + H_2O(\tilde{X})$ of the 1^1A_1 electronic symmetry will move to higher energy, showing an avoided crossing with the PES of the same symmetry correlating to $H + H_2O^+(\tilde{A})$.

This is shown in Figure 2 where, however, the geometries of H_2O and H_2O^+ are frozen, as discussed in section 2. For R distances in the neighborhood of the avoided crossing, the charge-transfer reaction 2 may therefore occur. The electron will transfer from the $3a_1$ MO, the tendency of this orbital to close the HOH bond angle will consequently be weakened, and the HOH angle will then open to the value of about 180°, which exists in $H_2O^{\bullet+}(\tilde{A})$ (see refs 10 and 12). We may now imagine that if the H• atom will more closely approach $H_2O^+(\tilde{A})$ in the same direction, a covalent bond will be formed. The electron density in $3a_1$ will thus increase because of the contribution of the added electron from the approaching H atom, and the HOH angle will get smaller than 180° passing through, say, the 120° of oxonium in D_{3h} geometry in an excited electronic state. Even here, more general directions of approach of H^+ to H_2O could be considered. Since the $H^+ + H_2O(\tilde{X})$ system is almost degenerate with the $H + H_2O^+(\tilde{A})$, an Rh configuration is probably not needed to allow an electron transfer with formation of $H + H_2O^+(\tilde{A})$. One should, moreover, consider that since $H_2O^+(\tilde{A})$ is linear and forms a well-known classical example of a Renner−Teller doublet with vibrationally excited linear $H_2O^+(v, \tilde{X})$, as may be seen from Figure 3a and 7a of a previous study of ours[10] as well as from Figure 1 of ref 12, we can find again $H_2O^+(v, \tilde{X})$ as an intermediate in a protonation process.

Finally, if H^+ approaches H_2O in the direction of an oxygen lone pair, i.e., in the C_s symmetry of Figure 3c that was employed by us to calculate the PEC of Figure 11 in ref 2, oxonium will be formed in its first excited electronic state, $H_3O^+(2^1A_1)$, and not, as one might naively suppose, in its ground electronic state.

The above analysis naturally leads us also to ask the question of what would happen when "pulling" a proton away from H_3O^+. If this were done following a C_s configuration, like in Figure 3c, one could cause a homolytic bond dissociation[21] that releases an electron to the proton as in eq 8. We would thus have a dehydrogenation of oxonium. To cause a deprotonation, i.e., a heterolytic bond dissociation as in eq 9, the system has to follow a path through the conical intersection or close to it, depending on the strength of the nonadiabatic coupling.

5. Discussion and Conclusions

The basis set used in the present work, albeit of medium size in view of the present state-of-the-art quantum chemical computations, was kept for consistency to be the same as that used in our previous computations.[2,7,9−11] Owing to the small energy difference between the asymptotic states $H^+ + H_2O(\tilde{X})$ and $H + H_2O^+(\tilde{A})$, very accurate electronic wave functions are needed for an exact localization of the avoided crossings between the two higher PES. Our rough evaluation of the likely localization of the avoided crossing and of its spacing only refers to a particular couple of PECs at a bent $H_2O^+(\tilde{A})$ configuration. Nonetheless, our qualitative analysis of the pattern of $\langle \Delta E_{tot}(\vartheta, \tilde{A}) \rangle$ does not depend on the exact localization of the avoided crossing but only on the existence of such a feature of the PECs. As a matter of fact, although one clearly keeps in mind the inherent complexity of the six-dimensional PESs involved in the processes examined, we believe that the present study, supported by specific "cuts" of accurately computed surfaces of lower dimensionality, is able to point out clearly two partially different physical mechanisms that are likely to play separate roles for the two charge-transfer channels considered in the molecular beam experiments of ref 1. The agreement shown in section 2 between theoretical predictions and experimental results lends support to our interpretation.

The existence of a crossing between the two lowest PECs for any arbitrary planar approach of H^+ to H_2O could have been surmised just by considering that every such configuration would be somehow between the Y and Rh configurations. This intuitive guess receives much better justification on the basis of the symmetry-based theoretical considerations discussed above. Actually, although detailed quantitative calculations will be necessary to find out the shape of the toroidal region encircling water in its molecular plane, we feel that its existence is likely to remain valid because of the above discussion on the water protonation. The latter, of course, is by no means a substitute for a full dynamical study of the process, although it provides an interesting enough illustration of the nonadiabaticity of the protonation process and of its charge-transfer aspects.

In conclusion, our present analysis is useful in describing the following overall chemical process:

$$H^+ + H_2O \leftarrow x \rightarrow [H_3O]^+ \leftrightarrow H + H_2O^+ \qquad (10)$$

where the double-pointed arrows indicate that the process could happen in both directions either on a single PES(↔) or on more than one PES through some curve-crossing mechanism (←x→).

Some recent results, closely related to ours, on the dissociation and the protonation of NH_3, the isoelectronic sister molecule of H_3O^+, were given by McCarthy et al.,[22] who found an $\tilde{X}-\tilde{A}$ conical intersection similar to the one here described, between the singlets $\tilde{X}$ and $\tilde{A}$ states of NH_3 correlated in planar structures with the $\tilde{A}$ and $\tilde{X}$ states of NH_2, respectively. Clear three-dimensional figures of the double-funnel shape of the conical intersection may be found in refs 18, 23, and 24. Two reviews recently appeared on this important topic.[25,26] Kaldor et al.[27] recently studied the protonation of ammonia leading to the formation of NH_4^+; Pelsatakis et al.[28] extended this work by further analyzing the charge-transfer aspect of the $H^+ + NH_3$ reaction. We found it interesting that Kaldor et al. did not find a crossing between PECs correlated to $H^+ + NH_3$ and $H + NH_3^+$ when the proton approaches ammonia along the direction jutting out of the N atom along the C_3 axis of the molecule. In our case we also did not find any nonadiabatic crossing when the proton approached H_2O in the C_s geometry.[2] In fact, since oxygen is the united atom of the NH group in the limit of zero nuclear separation of the two atoms,[14] contracting an NH group of NH_3 to an oxygen atom, we would have a geometry of approach of the proton to the NH_3 close to the one mentioned in ref 2 for the H_2O target!

Further studies on different systems bearing some similarities to the one examined here are currently being carried out in our group. We are presently analyzing the protonation of ozone[29] and that of LiH,[30] where both conical intersection and avoided crossing features are shown, by ab initio calculations, to be present at specific geometries.

Acknowledgment. E.E.N. acknowledges the support of the Elson/Shapiro families research fund. F.D.G. acknowledges a grant from the Deutsche Forschungsgemeinschaft and the

Consiglio Nazionale delle Ricerche for a stay in the fall of 1994 at the Department of Chemistry of Potsdam University with the kind hospitality of Professor L. Zülicke. E.E.N. and F.S. thank the University of Rome for an invitation to the Department of Chemical Engineering and Materials in the summer and fall of 1997. E.E.N. and F.D.G. also thank Prof. R. N. Compton, Prof. W. Jakubetz, Prof. W. Kutzelnigg, Prof. H. Lischka, Dr. B. Nestmann, and Prof. V. Staemmler for useful discussions and advice during the completion of the present work. F.A.G. acknowledges the support from the Max-Planck Gesellschaft as a 1995 research-prize awardee.

References and Notes

(1) Friedrich, B.; Niedner, G.; Noll, M.; Toennies, J. P. *J. Chem. Phys.* **1987**, *87*, 5256.
(2) Gianturco, F. A.; Raganelli, F.; Di Giacomo, F.; Schneider, F. *J. Phys. Chem.* **1995**, *99*, 64.
(3) Hedström, M.; Morales, J. A.; Deumens, E.; Öhrn, Y. *Chem. Phys. Lett.* **1997**, *279*, 241.
(4) Nikitin, E. E.; Ottinger, Ch.; Shalashilin, D. V. *Z. Phys. D* **1996**, *36*, 257.
(5) Nikitin, E. E.; Smirnov, B. M. *Slow Atomic Collisions*; Energoatomizdat: Moscow, 1990 (in Russian).
(6) Nikitin, E. E.; Umanskij, S. Ya. *Theory of Slow Atomic Collisions*; Springer: Berlin, 1984.
(7) Di Giacomo, F.; Gianturco, F. A.; Raganelli, F.; Schneider, F. *J. Chem. Phys.* **1994**, *101*, 3952.
(8) Griffiths, W. J.; Harris, F. M. *Int. J. Mass. Spectrom Ion Processes* **1988**, *85*, 339.
(9) Schneider, F.; Di Giacomo, F.; Gianturco, F. A. *J. Chem. Phys.* **1996**, *104*, 5153.
(10) Schneider, F.; Di Giacomo, F.; Gianturco, F. A. *J. Chem. Phys.* **1996**, *105*, 7560.
(11) Gianturco, F. A.; Schneider, F.; Di Giacomo, F. *Gazz. Chim. Ital.* **1995**, *125*, 361.
(12) Brommer, M.; Weis, B.; Follmeg, B.; Rosmus, P.; Carter, S.; Handy, N. C.; Werner, H. J.; Knowles, P. J. *J. Chem. Phys.* **1993**, *98*, 5222.
(13) Magee, J. L. *J. Chem. Phys.* **1940**, *8*, 687.
(14) Herzberg, G. *Molecular Spectra and Molecular Structure. III. Electronic Spectra and Electronic Structure of Polyatomic Molecules*; Van Nostrand Reinhold Company: New York, 1966.
(15) Landau, L. D.; Lifshitz, E. *Quantum Mechanics, Course of Theoretical Physics*; Butterworth-Heinemann: Oxford, 1997; Vol. 3.
(16) Teller, E. *J. Phys. Chem.* **1937**, *41*, 109.
(17) Nikitin, E. E. *Theory of Elementary Atomic and Molecular Processes in Gases*; Clarendon Press: Oxford, 1974.
(18) Schinke, R. *Photodissociation Dynamics*; Cambridge University Press: Cambridge, 1993.
(19) Casida, M. E.; Chen, M. M. L.; MacGregor, R. D.; Schaefer, H. F. *Isr. J. Chem.* **1980**, *19*, 127.
(20) Koga, T.; Nakatsuji, H.; Yonezawa, T. *Mol. Phys.* **1980**, *39*, 239.
(21) Wolf, J. W.; Staley, R. H.; Koppel, I.; Tangepera, M.; McIvery, R. T.; Beauchamp, J. L.; Taft, R. W. *J. Am. Chem. Soc.* **1977**, *99*, 5417.
(22) McCarthy, M. I.; Rosmus, P.; Werner, H. J.; Botschwina, P.; Vaida, V. *J. Chem. Phys.* **1987**, *86*, 6693.
(23) Dixon, R. N. *Mol. Phys.* **1989**, *68*, 263.
(24) Butler, L. J.; Neumark, D. M. *J. Phys. Chem.* **1996**, *100*, 12801.
(25) Yarkony, D. R. *Rev. Mod. Phys.* **1996**, *68*, 985.
(26) Yarkony, D. R. *Acc. Chem. Res.* **1998**, *31*, 511.
(27) Kaldor, U.; Roszak, S.; Hariharan, P. C.; Kaufman, J. J. *J. Chem. Phys.* **1989**, *90*, 6395.
(28) Petsalakis, I. D.; Theodorakopulos, G.; Nikolaides, C. A. *J. Chem. Phys.* **1994**, *100*, 5870.
(29) Ceotto, M.; Gianturco, F. A.; Hirst, M. In preparation.
(30) Bodo, E.; Gianturco, F. A.; Raimondi, M.; Sironi, M. In preparation.